

Functional Relevance of Urinary-type Plasminogen Activator Receptor (uPAR)- α 3 β 1 Integrin Association in Proteinase Regulatory Pathways

Supurna Ghosh¹, Jeffery J. Johnson¹, Ratna Sen¹, Shubhendu Mukhopadhyay¹, Yueying Liu¹, Feng Zhang³, Ying Wei³, Harold A. Chapman³ and M. Sharon Stack^{1,2,4}

¹Department of Cell & Molecular Biology, and

²Robert H. Lurie Comprehensive Cancer Center

Northwestern University Feinberg School of Medicine, Chicago, IL 60611 and

³Division of Pulmonary and Critical Care Medicine,
University of California, San Francisco, CA 94143

Running Title: Integrin regulation of proteinase expression

Address correspondence to: M. Sharon Stack, Dept of Cell & Molecular Biology, Northwestern University Feinberg School of Medicine, 303 E. Superior St., Lurie Bldg. 3-111, Chicago, IL 60611. Phone 312 908 8216, Fax 312 503 0386, Email: mss130@northwestern.edu

Squamous cell carcinoma of the oral cavity (OSCC) is characterized by persistent, disorganized expression of integrin α 3 β 1 and enhanced production of urinary-type plasminogen activator (uPA) and its receptor (uPAR) relative to normal oral mucosa. As multi-valent aggregation of α 3 β 1 integrin upregulates uPA and induces a dramatic co-clustering of uPAR, we explored the hypothesis that lateral ligation of α 3 β 1 integrin by uPAR contributes to uPA regulation in oral mucosal cells. To investigate mechanisms by which uPAR/ α 3 β 1 binding enhances uPA expression, integrin-dependent signal activation was assessed. Both src and ERK1/2 were phosphorylated in response to integrin aggregation and blocking src kinase activity completely abrogated ERK1/2 activation and uPA induction, whereas inhibition of EGFR tyrosine kinase activity did not alter uPA expression. Proteinase upregulation occurred at the transcriptional level and mutation of the AP1 (-1967) site in the uPA promoter blocked the uPAR/integrin-mediated transcriptional activation. As uPAR is redistributed to clustered α 3 β 1 integrins, the requirement for uPAR/ α 3 β 1 interaction in uPA regulation was assessed. Clustering of α 3 β 1 in the presence of a peptide (α 325) that disrupts uPAR/ α 3 β 1 integrin binding prevented uPA induction. Depletion of cell surface uPAR using siRNA also blocked uPA induction following integrin

α 3 β 1 clustering. These results were confirmed using a genetic strategy in which α 3 null epithelial cells reconstituted with wild type α 3 integrin, but not a mutant α 3 unable to bind uPAR, induced uPA expression upon integrin clustering, confirming the critical role of uPAR in integrin-regulated proteinase expression. Disruption of uPAR/ α 3 β 1 binding using peptide α 325 or siRNA blocked filopodia formation and matrix invasion, indicating that this interaction stimulates invasive behavior. Together these data support a model wherein matrix-induced clustering of α 3 β 1 integrin promotes uPAR/ α 3 β 1 interaction, thereby potentiating cellular signal transduction pathways culminating in activation of uPA expression and enhanced uPA-dependent invasive behavior.

Oral squamous cell carcinoma (OSCC) is the most common malignancy of the oral cavity, with a distinctly low (50%) 5-year survival rate (1). Advanced OSCC is associated with high mortality, resulting from local, regional and distant metastasis (2); however the cellular and biochemical factors that underlie OSCC dissemination are poorly understood. Recent studies have used cDNA microarray analysis for genome-wide monitoring of genetic and epigenetic changes associated with OSCC primary tumors and lymph node metastases. These studies have identified enhanced expression of the proteinase

urinary type plasminogen activator (uPA) and the cell-matrix adhesion molecule $\alpha 3$ integrin as key candidate biomarkers for prediction of poor disease outcome (3,4).

The serine proteinase uPA converts plasminogen to plasmin, a broad spectrum proteinase active against numerous matrix substrates and additional proteinase zymogens. Acquisition of uPA activity is the net result of regulatory interplay between uPA, its cell surface receptor (uPAR) and its physiological inhibitor, plasminogen activator inhibitor-1 (PAI-1) (5). These components have been extensively studied for their contribution to cell migration and invasion in various physiological and pathological conditions, particularly in cancer (6). The uPAR is a cell surface glycosyl phosphatidylinositol (GPI) anchored molecule that binds uPA and 'focalizes' proteolytic activity to the cell-matrix interface (7). Increased pericellular proteolysis of basement membrane proteins can then remove growth constraints imposed by the mechanical properties of a 3-dimensional matrix and potentiate invasion and metastasis (8-10). However, recent studies have identified other interesting biological functions of uPAR, including regulation of cell adhesion, proliferation and differentiation via interaction with other cell surface molecules including integrins and growth factor receptors (11-13). Recently published x-ray crystallography data suggest that uPAR does not undergo significant conformational changes upon uPA binding to its central cavity. Thus uPAR, bound to uPA in its central core, retains a large outer receptor surface accessible to additional binding partners such as integrins, which in turn may mediate other biological functions of uPAR (14).

Integrins are transmembrane heterodimeric proteins comprised of an α and a β subunit that mediate adhesion to matrix proteins through the extracellular domain and modulate signaling and cytoskeletal organization through the cytoplasmic tail. Numerous studies have demonstrated that the GPI-anchored uPAR can form lateral associations with transmembrane integrins (15-21), and uPAR/integrin binding has been shown to initiate or potentiate integrin signaling through focal adhesion kinase and/or src kinases, downstream to activate MEK/ERK pathways (13,18,19,22). These data support a mechanism whereby the GPI-anchored uPAR can

couple to cytoplasmic signaling pathways via binding to transmembrane integrins and thereby regulate gene expression and cell behavior (13).

While investigating the regulation of uPA activity in premalignant oral keratinocytes, we observed that multivalent aggregation of integrin $\alpha 3\beta 1$ upregulates uPA expression via a MEK/ERK1/2-dependent pathway, suggesting a mechanism whereby cell-matrix adhesion may regulate subsequent invasive behavior (23). Integrin clustering was accompanied by a redistribution of endogenous uPAR to sites of clustered $\alpha 3\beta 1$ integrins and formation of a uPAR/ $\alpha 3\beta 1$ complex as demonstrated using confocal immunofluorescence microscopy and co-immunoprecipitation analysis. This finding was supported by studies showing binding of exogenous uPAR to $\alpha 3\beta 1$ in 293 cells and identification of a peptide, designated $\alpha 325$, that blocks uPAR/ $\alpha 3\beta 1$ integrin binding (24). More recently, the uPAR binding site was mapped to loop 4 in the $\alpha 3$ subunit β -propeller region (residues 242-246) and a point mutation (H245A) in the $\alpha 3$ subunit was identified that abrogates uPAR binding (25). The objective of this study was to evaluate the functional contribution of uPAR/ $\alpha 3\beta 1$ interaction to regulation of uPA expression and activity. Our data support a model wherein matrix-induced clustering of $\alpha 3\beta 1$ integrin promotes uPAR/ $\alpha 3\beta 1$ interaction, thereby potentiating cellular signal transduction pathways culminating in enhanced uPA expression and uPA-dependent invasive behavior in premalignant oral keratinocytes.

MATERIALS AND METHODS

Materials: Plasminogen and plasmin were purified by affinity chromatography from outdated human plasma as described previously (23). Anti-human integrin $\alpha 3$ and $\beta 1$ monoclonal antibodies (P1B5 and P5D2) were obtained from Chemicon (Temecula, CA). Conformation specific anti- $\beta 1$ antibody (HUTS21) was obtained from BD Biosciences (Franklin Lakes, NJ). Affinity-purified polyclonal antibody specific for phosphorylated p42/p44 mitogen-activated protein kinase (anti-ACTIVE® MAPK p42/p44 or ERK1/2) was purchased from Promega (Madison, WI). Anti-ERK1/2 (anti-p42/p44) antibodies,

which recognize both phosphorylated and nonphosphorylated p42/p44, were obtained from Santa Cruz Biotechnology (Santa Cruz, CA). Phospho-src (Tyr416) antibody was obtained from Cell Signaling Technology (Beverly, MA). Pharmacological inhibitors of MEK1/2 (PD98059), src kinase (PP2), PI3K (LY294002), P38 MAPK (SB203580) and EGFR kinase (AG1478) were purchased from Calbiochem (San Diego, CA). Anti-human uPAR antibodies (3936, 3937, and 399R) and anti-catalytic uPA antibodies (394), were obtained from American Diagnostica (Greenwich, CT). Hydrobond-P polyvinylidene difluoride membrane and SuperSignal enhanced chemiluminescence reagents were obtained from Amersham Pharmacia Biotech and Pierce, respectively.

Cell Culture: HPV16 immortalized premalignant oral keratinocytes (pp126 cells) were a gift from Dr. D. Oda (University of Washington, Seattle, WA; (26). Telomerase reverse transcriptase-immortalized normal oral keratinocytes (OKF6/T cells) were kindly provided by Dr. J. Rheinwald (Brigham & Women's Hospital, Harvard Institutes of Medicine, Boston, MA) (27) and SCC25 cells derived from squamous cell carcinoma of the oral cavity were obtained from American Type Culture Collection (ATCC). pp126 cells were maintained in keratinocyte serum-free medium (Invitrogen) supplemented with 100 units/ml penicillin, 100 µg/ml streptomycin, 5 ng/ml epidermal growth factor, 50 µg/ml bovine pituitary extract supplied with the medium, and 0.09 mM CaCl₂. OKF6/T cells were maintained in keratinocyte serum-free medium supplemented with 100 units/ml penicillin, 100 µg/ml streptomycin, 25 µg/ml bovine pituitary extract (supplied with the medium), 0.2 ng/ml epidermal growth factor, and 0.31 mM CaCl₂. SCC25 were routinely maintained in Dulbecco's modified Eagle medium and Ham's F-12 medium (1:1) containing 10% fetal calf serum and supplemented with 100 units/ml penicillin and 100 µg/ml streptomycin.

A kidney epithelial cell line derived from α3 integrin-null mice, as well as these cells reconstituted with wild-type human α3 integrin and mutant (His245Ala) human α3 integrin were developed as previously described (25,28). α3

integrin deficient cells were cultured in DMEM supplemented with 10% FBS (Hyclone) and the α3-reconstituted cells were cultured in DMEM supplemented with 10% FBS and 50 µg/ml of zeocin (Invitrogen).

Prior to treatment with antibody-coated beads, cell monolayers were released from culture flasks by the addition of trypsin/EDTA, seeded at a constant density of 0.7×10^5 cells/well into 12-well tissue culture plates, and allowed to attach overnight in the medium described above. Cells were then washed twice with PBS, incubated for 15 h in medium lacking BPE and EGF, and supplemented with fresh BPE-/EGF-free medium prior to treatment with antibody-conjugated latex beads (20µl of bead slurry). Following incubation for the indicated time periods, conditioned media were collected for uPA activity determination. Alternatively, cell lysates were prepared using 50 mM Tris, 150 mM NaCl, 1% Nonidet P-40, 0.1% SDS (mRIPA). Total protein concentration of lysates was analyzed. In some experiments, inhibitors of signaling pathways including PD98039, PP2, AG1478, LY294002, SB203580 or DMSO (vehicle control) were added to culture wells 120 min prior to the introduction of integrin clustering beads. Cells were found to be >95% viable by exclusion of trypan blue at the highest concentrations of all the inhibitors used.

Preparation of antibody-coated latex beads:

Integrin antibodies and their IgG controls were covalently linked to 3.0 µm latex beads using a kit from Polysciences, Inc (Warrington, PA) following the manufacturer's instructions. In brief, 250 µl of 2.5% bead slurry (Polyscience Inc., Warrington, PA) was used for each batch bead preparation. Beads were washed in PBS and resuspended in 500 µl of 8% glutaraldehyde. The bead mixture was rotated for 4-6 hours at room temperature, centrifuged and washed thoroughly and finally resuspended in 700 µl PBS. 100 µg of antibody was added to the beads in PBS and incubated overnight on a rotator, following which beads were washed of excess, unbound antibodies, blocked with .2M ethanolamine and BSA and finally resuspended in 250 µl of storage buffer.

uPA activity assay: Net plasminogen activator activity in conditioned media was quantified using a coupled assay to monitor plasminogen activation and the resulting plasmin hydrolysis of a colorimetric substrate (D-Val-Leu-Lys-*p*-nitroanilide, Sigma) as described previously (23). Since the assay measures both uPA and tissue-type (tPA) plasminogen activator activity, control reactions contained 10 µg/ml of the anti-catalytic uPA antibody (American Diagnostica) to assess the level of tPA levels in cells. None of the oral cell lines tested expressed any tPA and all of the plasminogen converting activity in the conditioned medium was thus attributed to uPA.

uPA Promoter assays : p-uPA-CAT-2350 containing the sequence -2350 to +30 from the start site of the uPA gene was kindly provided by Dr. Douglas Boyd (MD Anderson Cancer Center, Houston, TX). The construct containing the uPA promoter was digested with *smal* and cloned into the *smal* site of the promoterless luciferase reporter vector pGL3 (Promega, Madison, WI) to generate the 2350 uPA-Luc construct. The clones were verified by sequencing. To generate the -1967 AP1-Luc, Quick-change site directed mutagenesis kit (Stratagene) was used. The oligonucleotides used to generate this mutation were: sense CCT CTT TGT CCA GGA AAT GAA aga ATC TGT CCT CAG CAA TCA GCA TGA, and antisense GTC ATG CTG ATT GCT GAG GAC AGA tct CTT CAT TTC CTC CTG GAC AA GAG G. The mutated bases are shown in lower case. The clones were verified by restriction digestion and confirmed by sequencing.

Subconfluent OKF6/T cells were grown in their normal growth medium and transfected with 2 µg of the reporter constructs using TransIT keratinocyte transfection reagent (Mirus, WI). Cells were then washed with growth factor free medium after 12 hours and treated with the integrin clustering beads coated with IgG, α3 or β1 integrin antibodies. After 18 hours, cells were washed with cold PBS, lysed and luciferase activities were determined by luminometry. The results were normalized to protein concentration and expressed relative to control cells.

Detection of p44/42 ERK and src Activation: To evaluate the phosphorylation state of ERK and

src, cells (0.7×10^5) were cultured overnight in growth factor-free medium followed by treatment with IgG, α3 or β1 coated beads as described above. At varying time points, cells were lysed with mRIPA buffer including 1 mM sodium orthovanadate and extracted on ice for 20 min. The lysates were centrifuged, protein concentration determined using the Bio-Rad protein assay kit, and equal amounts of cellular protein (20 µg) were electrophoresed on SDS-polyacrylamide gels and electroblotted to Immobilon. Blots were then probed with anti-ERK1/2 antibody (1:1000) to detect total ERK1/2 expression or with anti-ACTIVE-MAPK p42/p44 (1:2000) to detect the phosphorylated, active forms of ERK or anti-phospho src (1:1000) to estimate the level of active src.

Development of uPAR deficient OKF6/T cells:

An siRNA knockdown approach was used to generate cells with reduced levels of surface uPAR. The paired oligos indicated below were annealed and ligated to Bbs I cut vector (psiRNAhH1neo from Invivogen) and transformed into HB101 competent cells.

target	seq2	oligo	4A:
5'tccaagccgttacctcgaatgcatttcaagagaatgcattcgaggt			
aacggctttt 3';	target seq2	oligo	4B:
	5'caaaaaagccgttacctcgaatgcattctctgaaatgcattcgag		
	gtaacggctt 3'		

DNA was isolated (Qiaprep Spin Miniprep Kit, Qiagen) and the identities of the clones were confirmed by restriction digestion and sequencing with primer OL381 (sequencing primer oligo OL381: 5'ccctaaactgacacattcc 3'). Selected clones were then grown in 500 ml cultures and DNA isolations were done using a nuclease-free DNA isolation kit (Qiagen). OKF6/T cells were transfected by electroporation using the human keratinocyte nucleofactor kit and device (Amaxa) following the recommended protocol. Briefly, the cells were cultured to approximately 65% confluence, trypsinized, and resuspended at a density of 500,000 cells/100 µl nucleofactor solution. DNA (1.5 µg in less than 5 µl) was added to each aliquot of cells, gently mixed, and each aliquot was electroporated. After 24 hours under non-selective conditions, media was replaced with media containing 35 µg/ml G418. During outgrowth, cells were subcultured before reaching 70% confluence and selection media was replaced every 2 to 3 days. Colonies

were picked at the 100 cell stage, and grown until they were numerous enough to test for knockdown of uPAR by flow cytometry.

Flow cytometry: Surface expression of uPAR was determined using flow cytometry by incubating $1.8 \times 10^5/100 \mu\text{L}$ of medium containing antibodies against human uPAR (3937 from American Diagnostica, 1:100) for 45 minutes at room temperature. Cells were then washed twice with PBS and incubated with the corresponding fluorescein isothiocyanate (FITC)-conjugated secondary antibody (anti-mouse IgG FITC #GM488 from Molecular Probes, Eugene, OR) at a 1:1000 dilution for 30 minutes in the dark at room temperature. Cells were washed twice with PBS and resuspended in medium for fluorescence analysis on an Epics XL-MCL flow cytometer (Beckman Coulter, Hialeah, FL). Control experiments contained only the appropriate secondary antibody.

Cell Surface Biotinylation: Cells transfected with uPAR siRNA were grown in a 6-well plate, washed with ice-cold PBS, and incubated at 4°C with gentle shaking for 30 min with 0.5 mg/ml cell-impermeable Sulfo-NHS-Biotin in ice-cold PBS, followed by washing with 100 mM glycine to quench free biotin. Cells were then detached by scraping, lysed in modified RIPA buffer (50 mM Tris, pH 7.4, 150 mM NaCl, 5 mM EDTA, 1% Triton X-100, and 0.1% SDS) with proteinase inhibitors, and clarified by centrifugation. To isolate biotinylated cell-surface proteins, equal amounts of protein from each of the samples were incubated with streptavidin beads at 4°C for 14 h, followed by centrifugation. After boiling in Laemmli sample dilution buffer to dissociate streptavidin bead-biotin complexes, the samples were analyzed by SDS-PAGE (9% gels) and immunoblotted for uPAR (1:1000, American Diagnostica, clone 399R).

Analysis of Filopodial proteins: The relative localization of proteins in cellular vs filopodial fractions was evaluated following biochemical isolation of filopodia as described (29). Briefly, six well plates containing $1.0\mu\text{M}$ pore-size membrane inserts were coated on both top and bottom sides with rat-tail collagen (B.D

Biosciences, Catalog # 354236) to a concentration of $10 \mu\text{g/ml}$. The collagen was diluted with $0.1\text{M Na}_2\text{CO}_3$, pH 9.6 and kept overnight at 4°C for coating. Before the experiment, the inserts were washed twice with PBS. Near confluent dishes of OKF6/T cells were first serum starved overnight. The cells were then trypsinized and neutralized with soybean trypsin inhibitor, centrifuged and dissolved in serum free media. Cells (1×10^6) were then plated on top of each insert in growth factor free medium. Each bottom chamber contained 2.5 ml serum free media containing EGF ($.25\mu\text{g/ml}$) as a chemoattractant. Following a 12 h incubation (empirically determined based on the lack of visible nuclei in the 'bottom' fraction), total cell lysate was collected from top and bottom of paired inserts using lysis buffer (100mM Tris, 4.5 mM EDTA, 150mM NaCl, 1% SDS and protease inhibitor cocktail). The top and bottom lysates were collected and pooled from the replicate chambers, protein concentrations were determined and samples (40 ug) were then analyzed by Western blotting (29,30). The effect of peptide $\alpha 325$ or scrambled control peptide on filopodial protrusion was evaluated by performing the above assay in the presence of peptide ($20 \mu\text{M}$) followed by analysis of total filopodial protein as described above.

Analysis of Invasion: Invasive activity was quantified using a Boyden Chamber ($8 \mu\text{m}$ pore size) coated with Matrigel ($10 \mu\text{g}$ for 1 hour at room temperature) as described earlier (23,31). The cells (2×10^5) were added to the upper chamber in 500 μl of serum-free medium. Following 24 h incubation at 37°C , the non-invading cells were removed from the upper chamber with a cotton swab, filters were fixed and stained with Diff-Quik Stain, and invading cells adherent to the underside of the filter were enumerated using an ocular micrometer and counting a minimum of 10 high-powered fields. Data are expressed as relative migration (number of cells/field). Control experiments contained anti-catalytic uPA function blocking antibody (#394, American Diagnostica), uPAR blocking antibody (#3936, American Diagnostica), murine IgG (all antibodies 20 ug/ml) or exogenous uPA ($0.05 \mu\text{g/ml}$).

RESULTS

Adhesion-regulated proteinase expression.

Integrin clustering occurs at sites of cellular contact with 3-dimensional matrices, such as may be encountered by cells penetrating an extracellular matrix barrier (32,33). Integrins signal cellular responses by regulating the formation of signal transduction complexes on a cytoskeletal framework and this integration of signaling and cytoskeletal events is dictated by the physical nature of the integrin-ligand interaction. Low valency integrin occupancy can be induced by matrix protein fragments or soluble integrin subunit-specific antibodies and results in redistribution of the integrin to focal adhesions without activation of tyrosine kinase signaling or accumulation of cytoskeletal components (32,33). Integrin occupancy by a multivalent ligand such as presented by intact 3-dimensional extracellular matrix leads to a more robust cytoplasmic response characterized by the accumulation of a large variety of cytoskeletal (e.g., talin, α -actinin, paxillin) and signaling (e.g., Src, ERK, JNK) molecules at the cytoplasmic face of the integrin. This response can be mimicked by integrin subunit-specific antibodies immobilized on beads (32,33). We have previously demonstrated preferential adhesion of pre-malignant oral keratinocytes to laminin-5 and collagen I substrata via β 1 integrins, predominantly α 3 β 1 (23). Furthermore, culturing OKF6/T or pp126 cells in 3-dimensional collagen gels or in the presence of beads coated with type I collagen or laminin-5 results in a significant increase in uPA activity (not shown and ref. 23). Thus, to model cellular interaction with a 3-dimensional matrix that promotes multivalent α 3 β 1 integrin aggregation, integrin subunit-specific antibody coated beads were used to cluster α 3 β 1 integrins on the cell surface, followed by evaluation of uPA activity in conditioned medium as previously described (23,31,34). A significant increase in uPA activity was observed in the conditioned medium of premalignant pp126 and OKF6/T oral keratinocytes in response to α 3- or β 1-integrin clustering (Fig. 1 A, B), relative to IgG beads (grey bars) or untreated controls (open bars). In control experiments, neither soluble antibodies nor bead-immobilized antibodies directed against the

α 2, α 5, α 6, or β 4 integrin subunits altered uPA expression levels (ref. 23 and not shown).

To evaluate potential mechanisms by which integrin clustering may upregulate uPA expression, cells were treated with pharmacologic inhibitors of second messenger pathways known to be activated by integrin signaling. Following overnight culture in growth factor-free medium, cells were pre-incubated for 2 hours with specific inhibitors of MEK (PD98059, 50 μ M), src family kinases (PP2, 10 μ M), p38 MAPK (SB202190, 10 μ M), PI3K (LY294002, 10 μ M), EGF receptor tyrosine kinase (AG1478, 10 μ M) or DMSO control, followed by treatment with integrin antibody-beads for 22 hours to allow for accumulation of measurable uPA. Conditioned media were then collected, centrifuged and assayed for uPA activity. Similar responses were observed with both pp126 and OKF6/T cells and representative data from OKF6/T cells are shown (Figs. 2 and 3). Treatment of cells with both the MEK inhibitor PD98059 and the src inhibitor PP2 abrogated the production of uPA in response to α 3 β 1 integrin clustering (Fig. 2A and B). Clustering of integrin α 3 β 1 induced phosphorylation of both src (2.5-5.3-fold increase) and p44/42 ERK (3.0-4.6-fold increase) (Fig. 2C-F) and inhibition of src kinase activity with PP2 abrogated the phosphorylation of ERK1/2, implying that the activation of MEK is downstream of src kinase activity. In contrast, pharmacologic inhibitors of PI3K (LY294002) or p38 MAPK (SB202190) were ineffective in blocking α 3 β 1 integrin-induced uPA expression (Fig. 3A).

As β 1 integrin clustering can induce ERK1/2 phosphorylation via transactivation of the EGF receptor (EGFR) (35,36) and EGF treatment has been reported to induce uPA expression in many cell types including oral squamous cells (37-39), the role of EGFR transactivation in integrin-mediated uPA regulation was evaluated. In control experiments, EGF treatment increased uPA activity in pp126 cells and this induction was blocked by the EGFR tyrosine kinase inhibitor AG1478 (Fig 3B). In addition, clustering of α 3 β 1 integrin resulted in transactivation (phosphorylation) of the EGFR (not shown). However inhibition of EGFR kinase activity by AG1478 did not alter the upregulation of uPA

expression observed following integrin clustering (Fig 3C), suggesting independent pathways of uPA regulation by EGF and $\alpha 3\beta 1$ integrin.

ERK1 phosphorylation induces uPA promoter activation in oral SCC cells (40) and we previously reported that integrin-stimulated uPA expression is blocked by the general transcription inhibitor actinomycin D (23). To determine whether integrin-induced uPA expression was due to transcriptional activation of the uPA gene, luciferase reporter gene assays were performed using the sequence -2350 to +30 of the uPA promoter. OKF6/T cells were transiently transfected with the uPA promoter-luciferase construct, serum-starved overnight, and then treated with the $\alpha 3$ or $\beta 1$ antibody-coated or IgG control beads for an additional 18-20 h prior to lysis and measurement of luciferase activity. Regulation of uPA expression occurred at the transcriptional level, as clustering of $\alpha 3\beta 1$ integrin led to an increase in luciferase activity in cells transfected with the uPA promoter/luciferase reporter construct (Fig 4). Mutation of the AP-1 binding site (-1967), previously shown to be required for maximal ERK1-mediated promoter activation in squamous cells (40,41), blocked integrin-regulated transcriptional activation (Fig. 4). Basal promoter activity from untreated or IgG-bead-treated cells was unaffected by mutation of the AP-1 site (not shown).

uPAR is an essential contributor to integrin $\alpha 3\beta 1$ -induced uPA expression. Our results demonstrate that multi-valent aggregation of $\alpha 3\beta 1$ integrin leads to up-regulation of uPA expression via a src/MEK/ERK1-dependent pathway, suggesting a mechanism whereby matrix status may influence pericellular proteolytic potential. As integrin clustering also induces a dramatic redistribution of uPAR to sites of clustered integrins and formation of co-immunoprecipitable complexes between $\alpha 3\beta 1$ and uPAR (23), the requirement for direct uPAR/ $\alpha 3\beta 1$ integrin interaction in regulation of proteinase expression was evaluated using three distinct approaches. First, a blocking strategy was employed using a peptide derived from the W4 repeat region of $\alpha 3$ integrin ($\alpha 325$) that was demonstrated to block physical association between uPAR and $\alpha 3$ integrin and subsequent signaling events (24). It

was previously reported that peptide $\alpha 325$, but not homologous sequences from $\alpha 5$ or αv integrins, abrogated uPAR binding to recombinant $\alpha 3\beta 1$ (24), indicating that $\alpha 325$ specifically interferes with uPAR binding to $\alpha 3\beta 1$ integrin rather than other integrins. Cells were preincubated with $\alpha 325$ peptide or a scrambled sequence control (sc325) for 2 hours prior to addition of integrin antibody-coated beads. Clustering of $\alpha 3\beta 1$ in the presence of $\alpha 325$ abolished integrin-induced uPA expression (Fig. 5), suggesting that uPAR/ $\alpha 3\beta 1$ binding is required for initiation or potentiation of signaling events that lead to induction of uPA expression. The scrambled peptide had no effect on $\alpha 3\beta 1$ integrin-induced uPA expression (Fig. 5). In additional controls, clustering of uPAR alone, using bead-immobilized anti-uPAR antibodies, was not sufficient to induce uPA expression (not shown).

In the second approach, a genetic strategy was employed to test the functional contribution of uPAR/ $\alpha 3\beta 1$ integrin interaction to uPA regulation. Epithelial cells from mice genetically deficient in $\alpha 3$ integrin expression (28) were reconstituted with wild type or mutant human (H245A) $\alpha 3$ integrin. His 245 in the W4 repeat region of $\alpha 3$ integrin has been shown to be essential for uPAR/ $\alpha 3\beta 1$ complex formation and signaling (25). While the $\alpha 3$ -deficient R10 cells failed to respond to clustering (negative control, Fig. 6A), reconstitution of cells with wild-type human integrin $\alpha 3$ subunit restored integrin-regulated uPA expression (Fig. 6A). Furthermore, this induction was inhibited by the uPAR-blocking peptide $\alpha 325$, but not the scrambled control peptide sc325, (Fig. 6A). This result was confirmed by reconstitution of knockout cells with an $\alpha 3$ His245Ala mutant that retains the matrix binding site, but is incapable of forming complexes with uPAR (25). Although $\alpha 3$ antibody beads bound indistinguishably to cells expressing either wild type or H245Ala $\alpha 3$ and precipitated similar levels of the $\alpha 3$ integrin in control experiments (Figs. 6C and D), uPA expression was not induced in the His245Ala mutant reconstituted cells that lack uPAR/ $\alpha 3\beta 1$ lateral association (Fig. 6B), confirming the critical role of uPAR in integrin-regulated proteinase expression in this system.

Lastly, depletion of surface uPAR using siRNA was also used to examine the functional relevance of uPAR/ α 3 β 1 integrin interaction in proteinase induction. A relative decrease in surface uPAR of 30-60% was achieved using this strategy as quantified by FACS analysis (Fig. 7A and C) and surface biotinylation, shown for two representative clones in Fig. 7A. Downregulation of uPAR did not affect the surface levels of α 3 or β 1 integrins (Fig 7A) or alter basal uPA activity (data not shown). However significant changes were observed in responsiveness to integrin clustering as a result of uPAR knockdown. Whereas α 3 β 1 integrin clustering results in activation of ERK in untransfected (Fig. 2 C, D) or vector transfected cells (Fig. 7B), robust ERK activation was not observed in uPAR knockdown cells, shown for a representative clone (Fig. 7B, lane 4). Consistent with the lack of ERK1/2 phosphorylation, downregulation of surface uPAR also resulted in loss of uPA induction following α 3 β 1 integrin clustering (shown for 3 representative clones, Fig. 7C), further supporting the hypothesis that uPAR/ α 3 β 1 integrin interaction potentiates integrin signaling that control proteinase regulation pathways in response to microenvironmental cues.

Functional relevance of uPAR/ α 3 β 1 interaction. We have previously reported that uPA contributes to the invasive behavior of premalignant and malignant oral keratinocytes (23,31). Invasion of a three-dimensional matrix barrier is initiated by the protrusion of filopodia that serve as traction sites for migration (29). Activated integrins preferentially localize to the leading edge of the cell, initiate formation of focal adhesions, and transduce signals that regulate migration. Subsequent alterations in pericellular proteolytic potential can affect invasion of 3D matrices by removal of matrix constraints. Biochemical analysis of filopodial protrusions indicated that while uPAR is distributed relatively equally in the cellular *vs* filopodial fractions (Fig. 8A, second panel), α 3 integrin was preferentially localized in the filopodial pool (Fig. 8A, top panel). As the uPAR is also found in the filopodial fraction, the opportunity for uPAR/ α 3 β 1 interaction is likely substantially enhanced in this compartment. However, unlike α 3 integrin, the

entire population of cellular uPAR is not localized in filopodia, suggesting the existence of distinct cellular pools of uPAR. In control experiments, caveolin-1 was found in both the cellular and filopodial fractions, consistent with its localization in membrane lipid rafts (Fig. 8A, third panel) while PCNA was not detected in the filopodia fraction (not shown). Disruption of uPAR/ α 3 β 1 binding using peptide α 325 blocked filopodial protrusion, resulting in a 50% decrease in protein content in the filopodial fraction (Fig. 8B). As a consequence, a significant decrease in Matrigel invasion was observed in the presence of peptide α 325 (Fig. 8C), while the scrambled peptide sc325 has no effect on invasion (Fig. 8C). This is likely due to the loss of uPA induction, as function-blocking antibodies directed against both uPA and uPAR significantly inhibited invasion (Fig. 8D). A similar striking effect on invasive activity of malignant SCC25 cells is observed when comparing wild type to uPAR knockdown clones. In the representative experiment shown, a 6-fold decrease in invasive activity was observed relative to wild type cells (Fig. 8D) using a SCC25 uPAR knockdown clone with a 56% reduction in surface uPAR (as determined by FACS) and this is partially restored by addition of exogenous uPA, providing additional support for the hypothesis that uPAR/ α 3 β 1 interaction is an important regulator of cellular invasion.

DISCUSSION

Oral squamous cell carcinoma (OSCC) is the most common malignancy of the oral cavity, causing more deaths than any other oral disease. Approximately 30,000 new cases are diagnosed in the U.S. each year, resulting in patient deaths at a rate of 1 person/hour and the 5-year survival rate has not improved appreciably in over 20 years, remaining at a low 50% (1). These statistics reflect a limited understanding of the molecular events that govern disease progression. Thus, a more detailed analysis of the cellular and biochemical processes that contribute to OSCC metastasis is a necessary prerequisite to the development of novel early detection and treatment strategies that favorably impact survival of OSCC patients. To this end, recent studies have utilized cDNA microarray analysis for genome-wide monitoring

of genetic and epigenetic changes associated with OSCC primary tumors and lymph node metastases (3,4). These studies have identified the proteinase uPA and the cell-matrix adhesion molecule $\alpha 3$ integrin as key candidate biomarkers for prediction of poor disease outcome. The current data support these findings and suggest a functional link between $\alpha 3\beta 1$ integrin-mediated matrix interaction and acquisition of uPA-dependent pericellular proteolytic activity.

The normal oral mucosa is supported by a laminin-5-rich basement membrane overlaying a connective tissue stroma with loose reticular collagen III and VI and thick fiber bundles of collagen I (42,43). Hyperplastic premalignant lesions show enhanced laminin-5 staining intensity, while multifocal breaks in the basement membrane are observed in OSCC, indicative of proteolytic degradation (43,44). Laminin-5 is also observed in stromal tissues adjacent to budding carcinoma cells, suggesting that OSCC invasion is guided by the laminin-5 matrix (44). This hypothesis is supported by tissue culture models, wherein invading OSCC cells deposit laminin-5 at the matrix interface (45). Two cellular integrins interact with laminin-5, $\alpha 3\beta 1$ and $\alpha 6\beta 4$. While $\alpha 6\beta 4$ is involved in hemidesmosome formation (46), $\alpha 3\beta 1$ regulates adhesion, spreading and motility (47). Indeed, the $\alpha 3\beta 1$ /laminin-5 interaction was recently shown to be a major contributing factor to arrest of circulating tumor cells in the lung vasculature during pulmonary metastasis (48). This finding is consistent with the microarray data described above, as well as with studies of human OSCC tumors that demonstrate persistent, albeit disorganized, staining for $\alpha 3\beta 1$ integrin (49,50) and FACS analysis of OSCC cell lines that show enhanced $\alpha 3\beta 1$ integrin expression (31).

In addition to persistent expression of $\alpha 3\beta 1$ integrin, invasive and metastatic OSCC is also characterized by enhanced expression of uPA and its receptor uPAR relative to the normal oral mucosa. Highly invasive OSCC cells exhibit constitutive ERK activation, culminating in elevated basal uPA levels (31,40); however the cellular mechanisms that underlie dysregulated uPA expression in OSCC are not well-characterized. Previous studies demonstrated that uPA/R-integrin binding may modify integrin

function, providing a potential mechanism whereby the GPI-anchored uPAR may indirectly couple to cytoplasmic signaling pathways and thereby participate in regulation of gene expression, cell cycle progression, and/or motility (18,21). Our data support these findings and demonstrate that $\alpha 3\beta 1$ integrin clustering initiates a Src/MEK/ERK-dependent signaling pathway resulting in transcriptional activation of the uPA promoter. Complex formation between $\alpha 3\beta 1$ integrin and uPAR is necessary for integrin-induced uPA induction, as uPA expression is substantially attenuated by inhibition of $\alpha 3\beta 1$ /uPAR binding with peptide $\alpha 325$ (residues 241-257 of $\alpha 3$ integrin), siRNA downregulation of surface uPAR and expression of a mutated $\alpha 3$ subunit (H245A) that disrupts lateral association with uPAR.

The current data support the hypothesis that uPAR/ $\alpha 3\beta 1$ interaction potentiates integrin signaling for enhanced proteinase expression in response to integrin clustering. uPAR/integrin interaction has been previously demonstrated to alter the relative magnitude and duration of MAPK signaling, thereby altering tumor cell behavior [19]. Additional studies have shown that the ability of uPAR to function as a cis-acting ligand for $\alpha 3\beta 1$ leads to sustained low level activation of Src, in contrast with matrix engagement alone that promotes transient integrin signaling [25]. Together these data support a model wherein matrix-induced clustering of $\alpha 3\beta 1$ integrin promotes sustained uPAR/ $\alpha 3\beta 1$ interaction, thereby potentiating cellular signal transduction pathways culminating in activation of the uPA promoter. Further, we speculate that uPAR/ $\alpha 3\beta 1$ signaling is constitutively active in malignant OSCC (31), resulting in matrix-independent pericellular proteolysis and subsequent invasive behavior.

Acknowledgements: The authors would like to acknowledge the support of research grants RO1CA85870 (M.S.S.), PO1DE12328 (M.S.S.) and RO1HL44712 (H.A.C.) from the National Institutes of Health and from the H Foundation for basic science research (M.S.S.).

REFERENCES

1. www.NIH.gov.
2. Hicks, W. L., Jr., Loree, T. R., Garcia, R. I., Maamoun, S., Marshall, D., Orner, J. B., Bakamjian, V. Y., and Shedd, D. P. (1997) *Head Neck* **19**, 400-405
3. Nagata, M., Fujita, H., Ida, H., Hoshina, H., Inoue, T., Seki, Y., Ohnishi, M., Ohyama, T., Shingaki, S., Kaji, M., Saku, T., and Takagi, R. (2003) *Int J Cancer* **106**, 683-689
4. Al Moustafa, A. E., Alaoui-Jamali, M. A., Batist, G., Hernandez-Perez, M., Serruya, C., Alpert, L., Black, M. J., Sladek, R., and Foulkes, W. D. (2002) *Oncogene* **21**, 2634-2640
5. Myohanen, H., and Vaheeri, A. (2004) *Cell Mol Life Sci* **61**, 2840-2858
6. Andreasen, P. A., Egelund, R., and Petersen, H. H. (2000) *Cell Mol Life Sci* **57**, 25-40
7. Ploug, M. (2003) *Curr Pharm Des* **9**, 1499-1528
8. Yu, W., Kim, J., and Ossowski, L. (1997) *J Cell Biol* **137**, 767-777
9. Hotary, K. B., Allen, E. D., Brooks, P. C., Datta, N. S., Long, M. W., and Weiss, S. J. (2003) *Cell* **114**, 33-45
10. Andreasen, P. A., Kjoller, L., Christensen, L., and Duffy, M. J. (1997) *Int J Cancer* **72**, 1-22
11. Kugler, M. C., Wei, Y., and Chapman, H. A. (2003) *Curr Pharm Des* **9**, 1565-1574
12. Blasi, F., and Carmeliet, P. (2002) *Nat Rev Mol Cell Biol* **3**, 932-943
13. Ossowski, L., and Aguirre-Ghiso, J. A. (2000) *Curr Opin Cell Biol* **12**, 613-620
14. Llinas, P., Le Du, M. H., Gardsvoll, H., Dano, K., Ploug, M., Gilquin, B., Stura, E. A., and Menez, A. (2005) *Embo J* **24**, 1655-1663
15. Degryse, B., Resnati, M., Czekay, R. P., Loskutoff, D. J., and Blasi, F. (2005) *J Biol Chem* **280**, 24792-24803
16. Wei, Y., Czekay, R. P., Robillard, L., Kugler, M. C., Zhang, F., Kim, K. K., Xiong, J. P., Humphries, M. J., and Chapman, H. A. (2005) *J Cell Biol* **168**, 501-511
17. Xue, W., Mizukami, I., Todd, R. F., 3rd, and Petty, H. R. (1997) *Cancer Res* **57**, 1682-1689
18. Wei, Y., Lukashev, M., Simon, D. I., Bodary, S. C., Rosenberg, S., Doyle, M. V., and Chapman, H. A. (1996) *Science* **273**, 1551-1555
19. Aguirre Ghiso, J. A., Kovalski, K., and Ossowski, L. (1999) *J Cell Biol* **147**, 89-104
20. Pollanen, J., Hedman, K., Nielsen, L. S., Dano, K., and Vaheeri, A. (1988) *J Cell Biol* **106**, 87-95
21. Yebra, M., Goretzki, L., Pfeifer, M., and Mueller, B. M. (1999) *Exp Cell Res* **250**, 231-240
22. Nguyen, D. H., Catling, A. D., Webb, D. J., Sankovic, M., Walker, L. A., Somlyo, A. V., Weber, M. J., and Gonias, S. L. (1999) *J Cell Biol* **146**, 149-164
23. Ghosh, S., Brown, R., Jones, J. C., Ellerbroek, S. M., and Stack, M. S. (2000) *J Biol Chem* **275**, 23869-23876
24. Wei, Y., Eble, J. A., Wang, Z., Kreidberg, J. A., and Chapman, H. A. (2001) *Mol Biol Cell* **12**, 2975-2986
25. Zhang, F., Tom, C. C., Kugler, M. C., Ching, T. T., Kreidberg, J. A., Wei, Y., and Chapman, H. A. (2003) *J Cell Biol* **163**, 177-188
26. Oda, D., Bigler, L., Lee, P., and Blanton, R. (1996) *Exp Cell Res* **226**, 164-169
27. Rheinwald, J. G., and Beckett, M. A. (1981) *Cancer Res* **41**, 1657-1663
28. Wang, Z., Symons, J. M., Goldstein, S. L., McDonald, A., Miner, J. H., and Kreidberg, J. A. (1999) *J Cell Sci* **112 (Pt 17)**, 2925-2935
29. Cho, S. Y., and Klemke, R. L. (2002) *J Cell Biol* **156**, 725-736
30. Chodniewicz, D., and Klemke, R. L. (2004) *Exp Cell Res* **301**, 31-37
31. Ghosh, S., Munshi, H. G., Sen, R., Linz-McGillem, L. A., Goldman, R. D., Lorch, J., Green, K. J., Jones, J. C., and Stack, M. S. (2002) *Cancer* **95**, 2524-2533

32. Miyamoto, S., Akiyama, S. K., and Yamada, K. M. (1995) *Science* **267**, 883-885
33. Miyamoto, S., Teramoto, H., Coso, O. A., Gutkind, J. S., Burbelo, P. D., Akiyama, S. K., and Yamada, K. M. (1995) *J Cell Biol* **131**, 791-805
34. Munshi, H. G., Ghosh, S., Mukhopadhyay, S., Wu, Y. I., Sen, R., Green, K. J., and Stack, M. S. (2002) *J Biol Chem* **277**, 38159-38167
35. Kuwada, S. K., and Li, X. (2000) *Mol Biol Cell* **11**, 2485-2496
36. Liu, D., Aguirre Ghiso, J., Estrada, Y., and Ossowski, L. (2002) *Cancer Cell* **1**, 445-457
37. Ellerbroek, S. M., Hudson, L. G., and Stack, M. S. (1998) *Int J Cancer* **78**, 331-337
38. Shiratsuchi, T., Ishibashi, H., and Shirasuna, K. (2002) *J Cell Physiol* **193**, 340-348
39. Smith, P. C., Santibanez, J. F., Morales, J. P., and Martinez, J. (2004) *J Periodontal Res* **39**, 380-387
40. Lengyel, E., Gum, R., Stepp, E., Juarez, J., Wang, H., and Boyd, D. (1996) *J Cell Biochem* **61**, 430-443
41. Lengyel, E., Klostergaard, J., and Boyd, D. (1995) *Biochim Biophys Acta* **1268**, 65-72
42. Becker, J., Schuppan, D., Rabanus, J. P., Gelderblom, H. R., and Reichart, P. (1991) *Virchows Arch A Pathol Anat Histopathol* **419**, 237-244
43. Haas, K. M., Berndt, A., Stiller, K. J., Hyckel, P., and Kosmehl, H. (2001) *J Histochem Cytochem* **49**, 1261-1268
44. Kosmehl, H., Berndt, A., Strassburger, S., Borsi, L., Rousselle, P., Mandel, U., Hyckel, P., Zardi, L., and Katenkamp, D. (1999) *Br J Cancer* **81**, 1071-1079
45. Berndt, A., Hyckel, P., Konneker, A., Katenkamp, D., and Kosmehl, H. (1997) *Invasion Metastasis* **17**, 251-258
46. Jones, J. C., Dehart, G. W., Gonzales, M., and Goldfinger, L. E. (2000) *Microsc Res Tech* **51**, 211-213
47. Geuijen, C. A., and Sonnenberg, A. (2002) *Mol Biol Cell* **13**, 3845-3858
48. Wang, H., Fu, W., Im, J. H., Zhou, Z., Santoro, S. A., Iyer, V., DiPersio, C. M., Yu, Q. C., Quaranta, V., Al-Mehdi, A., and Muschel, R. J. (2004) *J Cell Biol* **164**, 935-941
49. Shinohara, M., Nakamura, S., Sasaki, M., Kurahara, S., Ikebe, T., Harada, T., and Shirasuna, K. (1999) *Am J Clin Pathol* **111**, 75-88
50. Sugiyama, M., Speight, P. M., Prime, S. S., and Watt, F. M. (1993) *Carcinogenesis* **14**, 2171-2176

FIGURE LEGENDS

Fig. 1. Integrin aggregation promotes uPA expression. Premalignant oral keratinocytes pp126 or OKR6/T, as indicated (0.7×10^5 cells/well of 12 well dish), were cultured for 15-18 hours and shifted to growth factor free medium for an additional 15 hours. Cells were then treated with 20 μ l of antibody- (IgG or $\alpha 3$ or $\beta 1$) coated latex beads or left untreated (designated '0'). After 22 hours, conditioned medium was collected and uPA activity was determined by a colorimetric assay.

Fig. 2. Induction of uPA activity by integrin clustering requires activation of ERK and src kinases. To identify the signaling pathways involved in integrin mediated induction of uPA activity, cells were cultured as described in Fig. 1 following pre-incubation with (A) MEK inhibitor PD98059 (10 μ M) or (B) src kinase inhibitor PP2 (10 μ M) or DMSO control (1:1000) for 2 hours. Cells were then treated with antibody- or IgG-coated beads, as indicated, in the continued presence of the inhibitors. Conditioned medium was collected after 22 hours and assayed for uPA activity (A,B). Alternatively, cells were lysed after 1.5 hours (C,D), total protein levels were determined and 20 μ g of protein was analyzed in western blot for phospho-ERK1/2 and phospho-src levels as described in Experimental Procedures. Blots were stripped and re-probed for total ERK or src as loading controls. Similar responses were observed with both pp126 and OKF6/T cells and representative data from OKF6/T cells are shown. (E,F) Semi-quantitative densitometric scanning of data in (D) normalized to total ERK levels.

Fig. 3. $\alpha 3\beta 1$ integrin-mediated induction of uPA activity does not require p38 MAPK, PI3K or EGFR kinase activities. (A) Following overnight culture in growth factor free medium, cells were pre-treated with DMSO (1:1000), P38MAPK inhibitor SB202190 (10 μ M) or PI3K inhibitor LY294002 (10 μ M). After 2 hours, cells were treated with designated antibody coated beads in continued presence of the inhibitors. After 22 hours, conditioned media were collected and assayed for uPA activity as described. (B,C) Cells were cultured for 15 hours without growth factors, pre-treated with EGFR kinase inhibitor AG1478 where indicated (AG) for 2 hours, and then treated with either 10nM EGF (B) or 20 μ l IgG- or $\beta 1$ integrin-antibody coated beads (C). After 22 hours, conditioned media were assayed for uPA activity. Similar responses were observed with both pp126 and OKF6/T cells and representative data from OKF6/T cells are shown.

Fig 4. Integrin $\alpha 3\beta 1$ induces transcriptional activation of the uPA promoter via the -1967 AP1 site. OKF6/T cells were transiently transfected with a uPA promoter/luciferase construct (-2350 to +30), either wild type (top bars) or mutated at the AP1 site (-1967, bottom bars). After 14 h of transfection, cells were washed and incubated in growth factor free medium for an additional 8 hours, followed by treatment with IgG- or integrin antibody coated beads as indicated. After 18 h, cell lysates were evaluated for luciferase activity as described in Experimental Procedures.

Fig. 5. Disruption of $\alpha 3\beta 1$ /uPAR interaction abolishes integrin-mediated induction of uPA activity. OKF6/T cells were pre-incubated in the presence of $\alpha 325$ peptide (20 and 40 μ M as indicated) to disrupt uPAR/ $\alpha 3$ integrin binding, equal concentration of scrambled peptide, or 1:1000 dilution of vehicle control (DMSO) for 2 hours. Following preincubation, cells were treated with bead immobilized IgG or $\alpha 3$ integrin antibodies, as indicated, in the continued presence of the peptides. After 22 h, conditioned media were assayed for uPA activity using a coupled colorimetric assay.

Fig. 6. Analysis of murine $\alpha 3^{-/-}$ cells reconstituted with wild-type and mutant human $\alpha 3$ integrin. (A) Epithelial cells from $\alpha 3^{-/-}$ mice and the same cells stably transfected with human $\alpha 3$ integrin (25) were treated with beads coated with IgG or anti- $\alpha 3$ antibodies as described above and 22 h conditioned media were assayed for uPA activity. Results are normalized relative to IgG-bead treated cells (designated 1).

Pre-treatment with peptide $\alpha 325$ (40 μM), but not the scrambled control abrogates uPA induction in response to integrin clustering. **(B)** $\alpha 3^{-/-}$ murine epithelial cells stably transfected with wild type (Hu- $\alpha 3$) or mutant (Hu- $\alpha 3$ -H245A) $\alpha 3$ integrin were treated with beads coated with IgG or anti- $\alpha 3$ antibodies and conditioned media were analyzed as described above. Changes in uPA activity are expressed as fold difference from the IgG-bead control. **(C)** $\alpha 3^{-/-}$ murine epithelial cells stably transfected with wild type (Hu- $\alpha 3$) or mutant (Hu- $\alpha 3$ -H245A) $\alpha 3$ integrin were incubated with $\alpha 3$ integrin antibody-beads or isotype-matched control IgG beads and examined visually using phase-contrast microscopy. Integrin $\alpha 3$ subunit antibody-coated beads bound avidly (b,d) to cells reconstituted with both wild type (b) and H245A mutant $\alpha 3$ integrin (d), relative to loosely adherent IgG control beads (a,c). Similar results were obtained using premalignant oral keratinocytes (23). **(D)** Murine epithelial cells treated with IgG- or anti- $\alpha 3$ -integrin-beads were lysed with mRIPA buffer and beads were precipitated by centrifugation, washed with PBS and analyzed by western blotting to demonstrate that the relative efficiency of $\alpha 3$ integrin antibody-bead binding to either wild type or H245A-mutant $\alpha 3$ integrin is identical.

Fig.7. Downregulation of uPAR expression blocks integrin-mediated uPA induction. **(A)** Vector control and uPAR siRNA expressing clones (KD7 and KD51) were cultured on 6 well dishes and surface-labeled with cell-imperable Sulfo-NHS-Biotin. Labeled proteins were then precipitated with streptavidin (Experimental Procedures) and surface uPAR and $\beta 1$ integrin expression levels were analyzed by western blotting. Relative surface expression levels of $\alpha 3$ integrin and uPAR were also measured by flow cytometric analysis using primary antibodies P1B5 and 3937, respectively, and GM488 secondary antibody and mean fluorescence index values are shown. Note that while relative uPAR levels are downregulated, relative levels of $\alpha 3$ integrin expression are not altered by uPAR siRNA. **(B)** A representative vector control and a uPAR knockdown clone were treated with beads coated with control IgG or anti- $\alpha 3$ integrin antibody for 1.5 h prior to lysis and immunoblotting with antibodies directed against phospho-ERK (P-ERK) or total ERK1/2 as indicated. **(C)** Vector control (V22, V29) or uPAR knockdown clones (KD7, KD11, KD51) were treated with bead-immobilized IgG, anti- $\alpha 3$, or anti- $\beta 1$, as indicated and 22 h conditioned media were assayed for uPA activity. All knockdown clones had a 30-60% decrease in surface uPAR, as quantified by FACS (indicated below the clone numbers). Results are normalized relative to V22/IgG control (designated 1).

Fig. 8. Functional relevance of uPAR- $\alpha 3\beta 1$ interaction. **(A)** OKF6/T cells were seeded onto a tissue culture insert containing a porous membrane (1 μm pores) coated on the underside with type I collagen. After 12 h, filopodial protrusions were purified by scraping the underside of the membrane, solubilized and analyzed for protein concentration. An equal amount (40 μg) of filopodial (bottom) or total cellular (top) protein was evaluated by western blotting for $\alpha 3$ integrin, uPAR, caveolin-1 and GAPDH. **(B)** OKF6/T cells were seeded onto a tissue culture insert containing a porous membrane (1 μm) in the presence or absence of peptide $\alpha 325$ (white bar) or control scrambled peptide (black bar), as indicated. After 12 h, filopodial protrusions were purified and filopodial protein content quantified. Results are presented relative to control untreated cells (grey bar, designated '1'). **(C)** OKF6/T cells were plated in the top of a Boyden chamber (8 μm pore size, coated with Matrigel) with peptide $\alpha 325$ (white bar) or control scrambled peptide (black bar). After 36 hours, invading cells at the bottom chamber were stained and enumerated. Data are expressed as % invasion relative to untreated control (grey bar, designated 100%). **(D)** Representative clones of vector control and uPAR knockdown (KD) SCC25 cells were added to the top of Matrigel-coated Boyden chambers in the presence or absence of anti-catalytic uPA antibody (designated uPA Ab), function blocking uPAR antibody (designated uPAR Ab) or exogenous uPA (0.05 $\mu\text{g}/\text{ml}$), as indicated. Invasion was evaluated as in (C). Results are shown as % invasion relative to vector control (designated 100%).

Fig.1

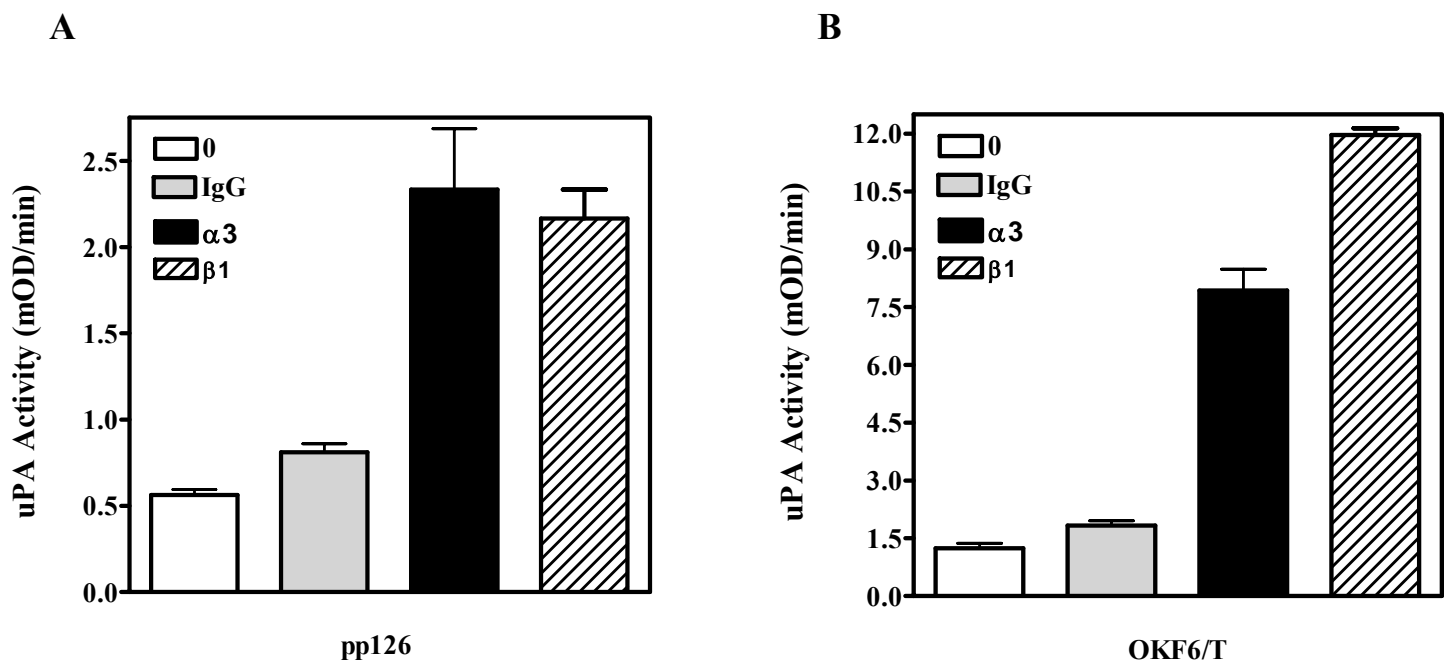


Fig. 2

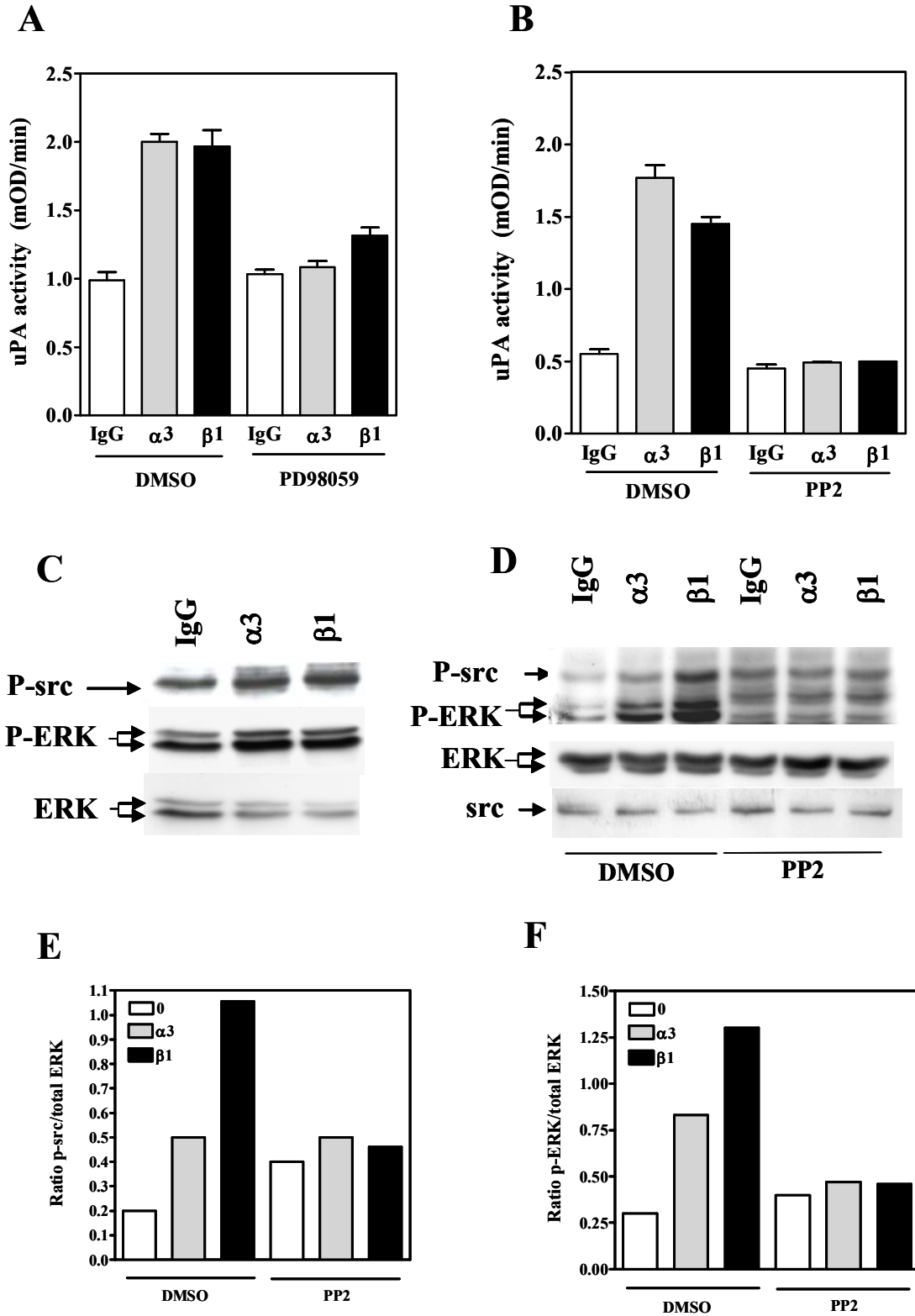


Fig 3

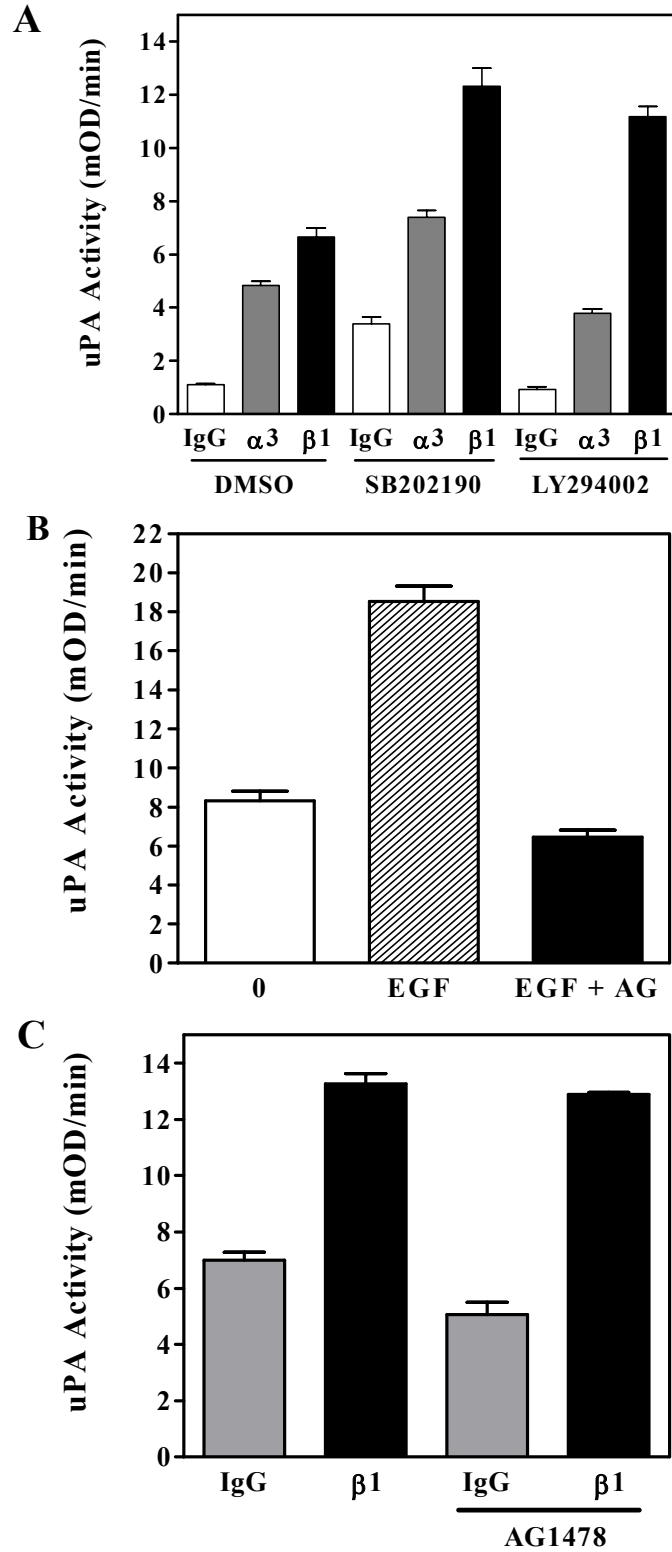


Fig.4

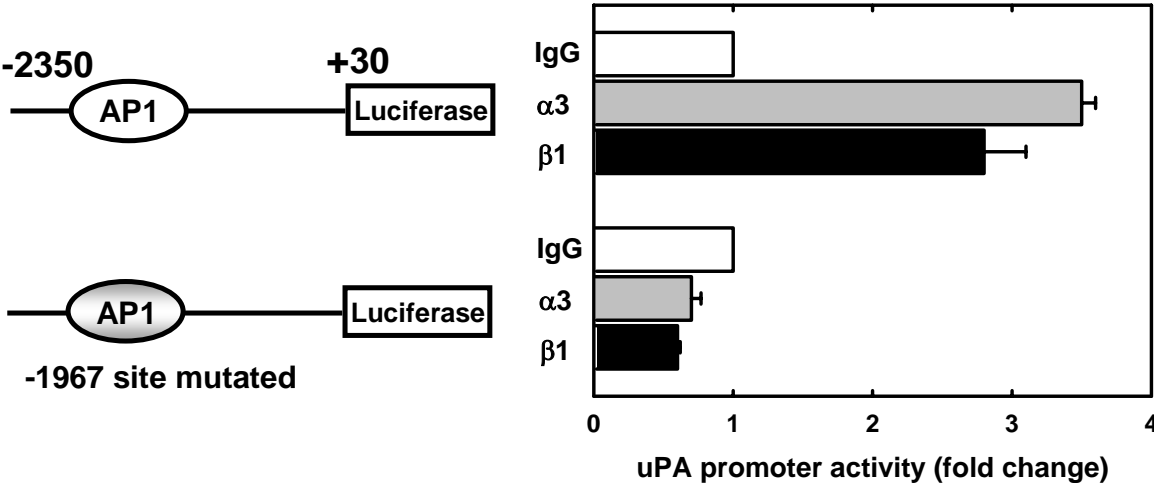


Fig.5

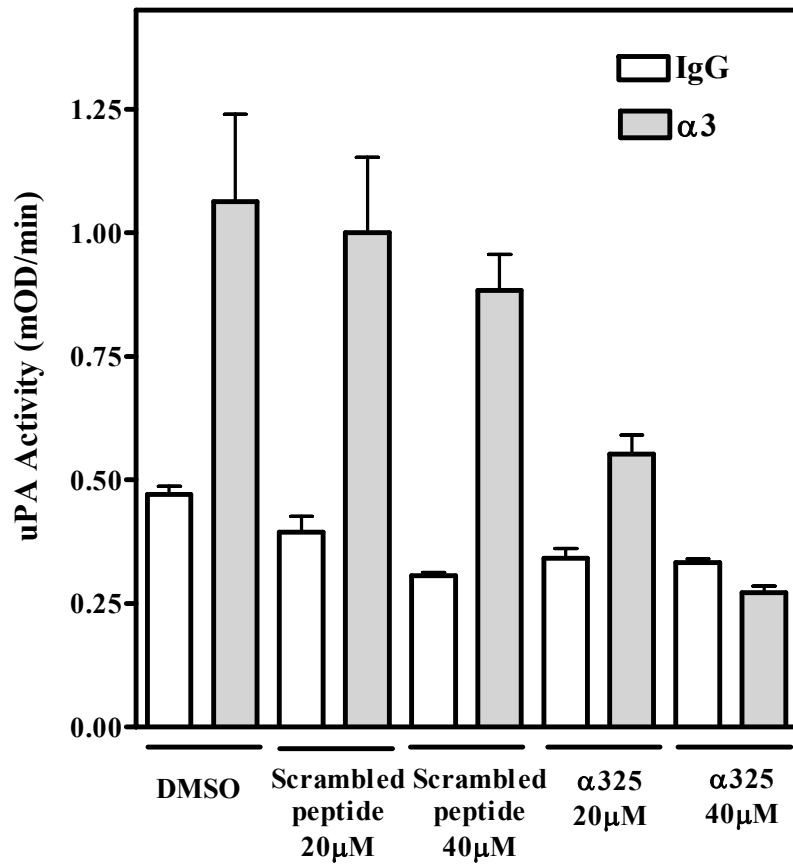


Fig.6

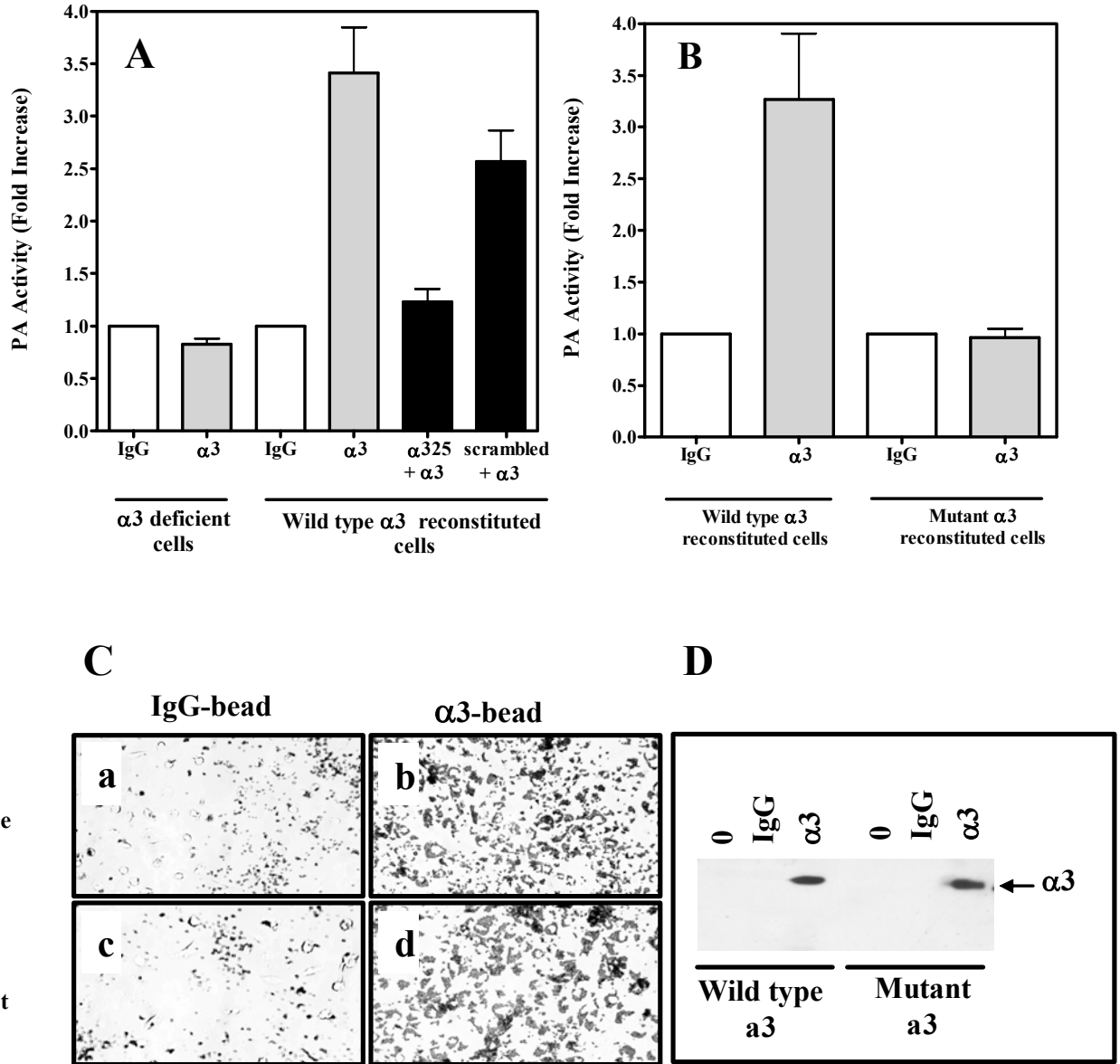


Fig.7

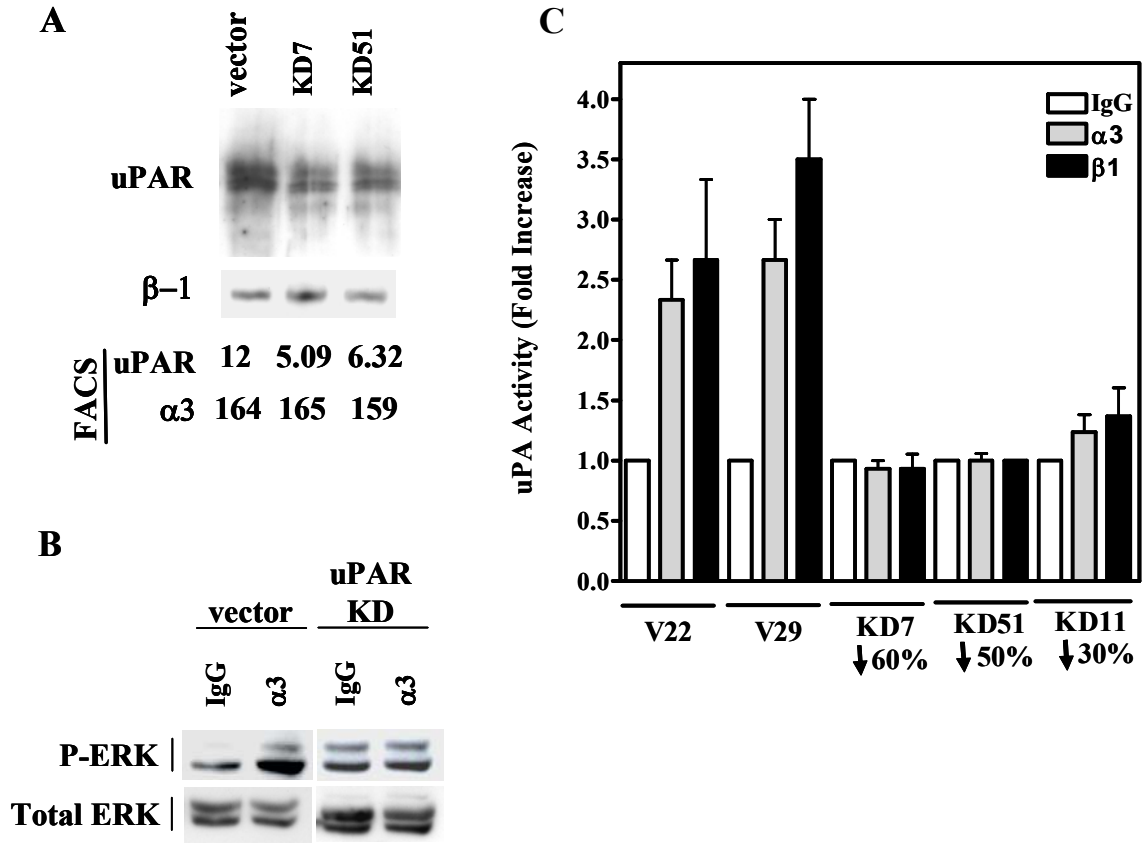


Fig.8

